Earth and Planetary Science Letters 329–330 (2012) 1–10

Contents lists available at SciVerse ScienceDirect

Earth and Planetary Science Letters

journal homepage: www.elsevier.com/locate/epsl

Influence of magmatism on mantle cooling, surface heat flow and Urey ratio

Takashi Nakagawa [a,*], Paul J. Tackley [b]

[a] Institute for Research on Earth Evolution, Japan Agency for Marine-Earth Science and Technology, Yokohama, Japan
[b] Institute of Geophysics, Department of Earth Sciences, ETH Zurich, Switzerland

ARTICLE INFO

Article history:
Received 4 November 2011
Received in revised form 4 February 2012
Accepted 11 February 2012
Available online 22 March 2012

Editor: Y. Ricard

Keywords:
Urey ratio
surface heat flow
heat production
partial melting
mantle convection

ABSTRACT

Two-dimensional thermo-chemical mantle convection simulations are used to investigate the influence of melting-inducted differentiation on the thermal evolution of Earth's mantle, focussing in particular on matching the present-day surface heat flow and the 'Urey ratio'. The influence of internal heating rate, initial mantle temperature and partitioning of heat-producing elements into basaltic crust are studied. High initial mantle temperatures, which are expected following Earth's accretion, cause major differences in early mantle thermo-chemical structures, but by the present-day surface heat flux and internal structures are indistinguishable from cases with a low initial temperature. Assuming three different values of mantle heat production that vary by more than a factor of two results in small differences in present-day heat flow, as does assuming different partitioning ratios of heat-producing elements into crust. Indeed, all of the cases presented here, regardless of exact parameters, have approximately Earth's present-day heat flow, with substantial fractions coming from the core and from mantle cooling. As a consequence of the model present-day surface heat flow varying only slightly with parameters, the Urey ratio (the ratio of total heat production to the total surface heat flow) is highly dependent on the amount of internal heat production, and due to the large uncertainty in this, the Urey ratio is considered to be a much poorer constraint on thermal evolution than the heat flow. The range of present-day Urey ratio observed in simulations here is about 0.3 to 0.5, which is consistent with observational and geochemical constraints (Jaupart et al., 2007). Magmatic heat transport contributes an upper bound of 9% to Earth's present-day heat loss but a much higher fraction at earlier times —often more than convective heat loss—so neglecting this causes an overestimation of the Urey ratio. Magmatic heat transport also plays an important role in mantle cooling. Considering these points, it is important to include magmatic effects when attempting to understand the thermal evolution of the Earth.

1. Introduction

The surface heat flow is arguably the most important constraint on the thermal evolution of Earth's mantle. A typical estimate of the present-day total surface heat flow is 46 TW (e.g. Jaupart et al., 2007). It is useful to decompose this into oceanic and continental parts: the surface heat flow through oceanic lithosphere is 32 TW and that from the mantle is 39 TW (Jaupart et al., 2007) which, when averaged over the entire surface, correspond to heat fluxes of 62 mW/m^2 and 76 mW/m^2 respectively. In our previous study on the thermal evolution of Earth's mantle and core (Nakagawa and Tackley, 2010), the model surface heat flow was around 20 TW, which is a factor of 1.5 lower than Earth's oceanic heat flow. A major reason for this is that the convective vigour was lower than Earth-like, which was partly because the assumed reference viscosity of 10^{22} Pa s is higher than the value constrained by post-glacial rebound and other observations (Barnhoorn et al., 2011; Haskell, 1935; Mitrovica and Forte, 2004; Peltier, 1996).

Previous thermal evolution studies have often focussed on the Urey ratio, which is the ratio of total heat production to the surface heat flow. Combining constraints on surface heat flow with geochemical constraints on mantle heat production leads to a Urey ratio estimate in the range of 0.21 to 0.49 (Jaupart et al., 2007); another review places it at 0.08–0.38 (Korenaga, 2008). A long-standing problem is, however, that in parameterised models of thermal evolution that use standard Nusselt number–Rayleigh number scaling (e.g. (Davies, 1980; Turcotte, 1980)), or in fully dynamical simulations of convection (e.g. Butler, 2009; Deschamps et al., 2010; Honda and Iwase, 1996), the Urey ratio is found to be significantly higher than this, creating a paradox in understanding Earth's thermal history. Early on, Christensen (1985) recognised that a low exponent in the Nusselt number–Rayleigh number scaling (i.e. β in Nu–Ra^{β}) provided a solution to this problem, and noted that this is characteristic of convection with moderately temperature-dependent viscosity, although it was subsequently argued (Gurnis, 1989) that when plates are correctly included, β reverts to the standard value of ~0.3. More recently it was proposed that accounting for the dissipation due to slab

* Corresponding author.
E-mail address: ntakashi@jamstec.go.jp (T. Nakagawa).

0012-821X/$ – see front matter © 2012 Elsevier B.V. All rights reserved.
doi:10.1016/j.epsl.2012.02.011

bending produces a lower value of β (Conrad and Hager, 1999) particularly when dehydration strengthening is included (Korenaga, 2006; Korenaga, 2008), and although a crucial component of this scaling—constant slab bending radius—is arguably invalid (as argued by Davies (2009) and Leng and Zhong (2010) and observed by Buffett and Heuret (2011)), isochemical numerical convection calculations (Korenaga, 2010) do indicate a substantial effect of dehydration strengthening on the heat flow scaling. However, thermal evolution when both plate-like behaviour and material differentiation due to partial melting are included is difficult to predict analytically because both effects, in particular plate-like behaviour, are strongly dependent on the horizontal length-scale and time (e.g. Grigne et al., 2005, 2007; Labrosse and Jaupart, 2007). Moreover, including dense compositional layers or 'piles' above the core–mantle boundary can substantially alter the thermal history due to buffering of heat from the core (Nakagawa and Tackley, 2004, 2005), storage of heat-producing elements in the dense material (Coltice et al., 2000), and temporal transitions in the style of layering (e.g. Davaille, 1999; Gonnermann et al., 2002). These factors seriously limit the applicability of parameterized approaches to studying the thermal evolution of Earth's mantle.

The presence of continental lithosphere also likely has a large influence, with (Lenardic et al., 2011) finding out that the mantle heat loss would be roughly the same if continents were removed and their heat-producing elements mixed into the mantle, arguing that a Urey ratio of 0.21 to 0.49 with continents is equivalent to a Urey ratio of 0.33 to 0.76 without continents. Continents also influence the horizontal length-scale (e.g. Grigne et al., 2007), which influences heat loss (Grigne et al., 2005). Considering these various influences on the scaling of convective heat transfer, it is best to study the thermal evolution of Earth's mantle using fully dynamical models that include both plate-like behaviour and melt-induced differentiation. Ogawa (2007) studied how the radiogenic internal heating rate in the mantle affects the evolution of thermo-chemical structures in mantle convection simulations that include melt migration, and found that present-day seismic tomographic observations are best matched by an internal heating rate that is not very large. However, the Urey ratio was not studied in this paper and the model was in a 2-D rectangular box, in which the relative areas of surface and CMB and the ratio of surface area to mantle volume are not correctly reproduced.

In order to estimate the Urey ratio, the internal heating rate in the mantle is required. This has been estimated using geochemical analyses (e.g. Lyubetskaya and Korenaga, 2007; McDonough and Sun, 1995), measurements of geoneutrinos (The KamLand Collaboration, 2011) and by inferring the heating rate needed to explain the observed surface heat flow (Schubert et al., 2001). The estimates for bulk silicate Earth range from 10 to 30 TW. Assuming that the amount of heat production in the continental crust is 7.5 TW (Rudnick and Gao, 2003), the range of heat production in Earth's mantle is approximately 3 TW to 28 TW, which is a huge range. Thus, it is important to test the influence of heat production rate on mantle evolution.

Here we study the thermal evolution of Earth's mantle and core, including melt-induced silicate differentiation, plate-like behaviour and a global core heat balance. We investigate the model evolution as a function of heat production rate, initial mantle temperature and partitioning of heat-producing elements into the basaltic component. We study the Urey ratio that incorporates heat loss by both conduction and magmatism (heat pipe mechanism), and find that our results are consistent with the estimated surface heat loss and Urey ratio for the Earth.

2. Model description

A coupled model, in which a 2-D thermo-chemical mantle convection calculation is coupled to a parameterized core heat balance, is used here. The model is very similar to that used in our previous papers (Nakagawa and Tackley, 2004, 2005, 2010). In Nakagawa and Tackley (2010) we found that the thermo-chemical evolution obtained using 2-D spherical annulus geometry (Hernlund and Tackley, 2008) is very similar to that obtained in a full 3-D spherical shell; therefore the present models use a 2-D spherical annulus. To summarize: The compressible truncated anelastic approximation is assumed, with the material properties thermal expansivity and thermal conductivity dependent on depth. Viscosity is dependent on both temperature and depth, and undergoes plastic yielding to mobilize the lithosphere with a surface yield stress of 120 MPa, given by:

$$\begin{aligned}\eta_d &= A_0\left(\prod_{ij}\Delta\eta_{ij}^{\Gamma_{ij}f_j}\right)\exp[9.1535(0.5-z)]\exp\left[\frac{32.716}{T+0.88}\right]\\ \eta_Y &= \frac{\sigma_0+\sigma_1(1-z)}{2\dot{\varepsilon}}\\ \eta &= \left(\frac{1}{\eta_d}+\frac{1}{\eta_Y}\right)^{-1}\end{aligned} \tag{1}$$

where A_0 is the prefactor calculated such that the nondimensional viscosity is one at T = 0.64 (corresponding to 1600 K) and z = 0.5, $\Delta\eta_{ij}$ is the viscosity change at the various phase transitions, which is 1 for all except for the phase transition to perovskite + magnesiowüstite at around 660 km depth where it is set to 30, Γ_{ij} is the phase function (between 0 and 1), f_j is the fraction of phase system j present, σ_0 is the yield stress at the surface (120 MPa), σ_1 is the yield stress gradient (0.064 MPa/km) and $\dot{\varepsilon}$ is the second invariant of the strain-rate tensor. Here a viscosity reduction due to the post-perovskite phase, which can influence the CMB heat flux (Nakagawa and Tackley, 2011), is not included because we focus instead on the influence of radiogenic heat production and magmatism. A difference from our previous thermal evolution models (Nakagawa and Tackley, 2010) is the depth at which the reference viscosity is defined. In the previous study, the reference viscosity was defined at zero pressure. Here it is defined at the mid-depth of mantle. This lowers the viscosity by approximately an order of magnitude (at each temperature and depth) increasing the effective Rayleigh number accordingly.

To solve the equations of thermo-chemical multiphase mantle convection in a 2-D spherical annulus and hence simulate thermal history of both mantle and core we use the numerical code StagYY (Tackley, 2008; Hernlund and Tackley, 2008). Rock mineralogy is decomposed into the olivine system and the pyroxene–garnet system, the proportions of which depend on local composition. The density profiles for the olivine and pyroxene–garnet system are plotted in Fig. 1 of Nakagawa and Tackley (2010); for pyroxene the intermediate density profile is assumed here. Rock is assumed to be a mixture of basalt and harzburgite (e.g. as in Xu et al. (2008)), with the field C representing the fraction of basalt at each location. This is converted to phase fraction assuming that basalt is pure pyroxene–garnet whereas harzburgite is 3/4 olivine and 1/4 pyroxene–garnet. If the local temperature exceeds a depth-dependent solidus (plotted in Fig. 1 of Nakagawa and Tackley (2004)) enough basaltic melt is generated to bring the temperature back to the solidus assuming a latent heat of 625 kJ/kg and this melt is immediately erupted at the surface to form oceanic crust. Only melt generated in the upper mantle can erupt; we also tried limiting the maximum eruption depth to 300 km but this made a negligible difference to the thermal history. The composition of basalt does not change with degree of melting and if no solid basalt exists at a particular location, no melting is possible there. Subsequent segregation of subducted crust above the CMB generates compositional anomalies in this region. A numerical resolution of 1024 × 128 cells, with 30 tracers per cell to track composition, is used. The initial CMB temperature is assumed to be 6000 K, and 400 ppm of radioactive potassium in the core is assumed, because this combination produced one of the "best-fit" scenarios (for explaining both the inner core size and the existence of long-term

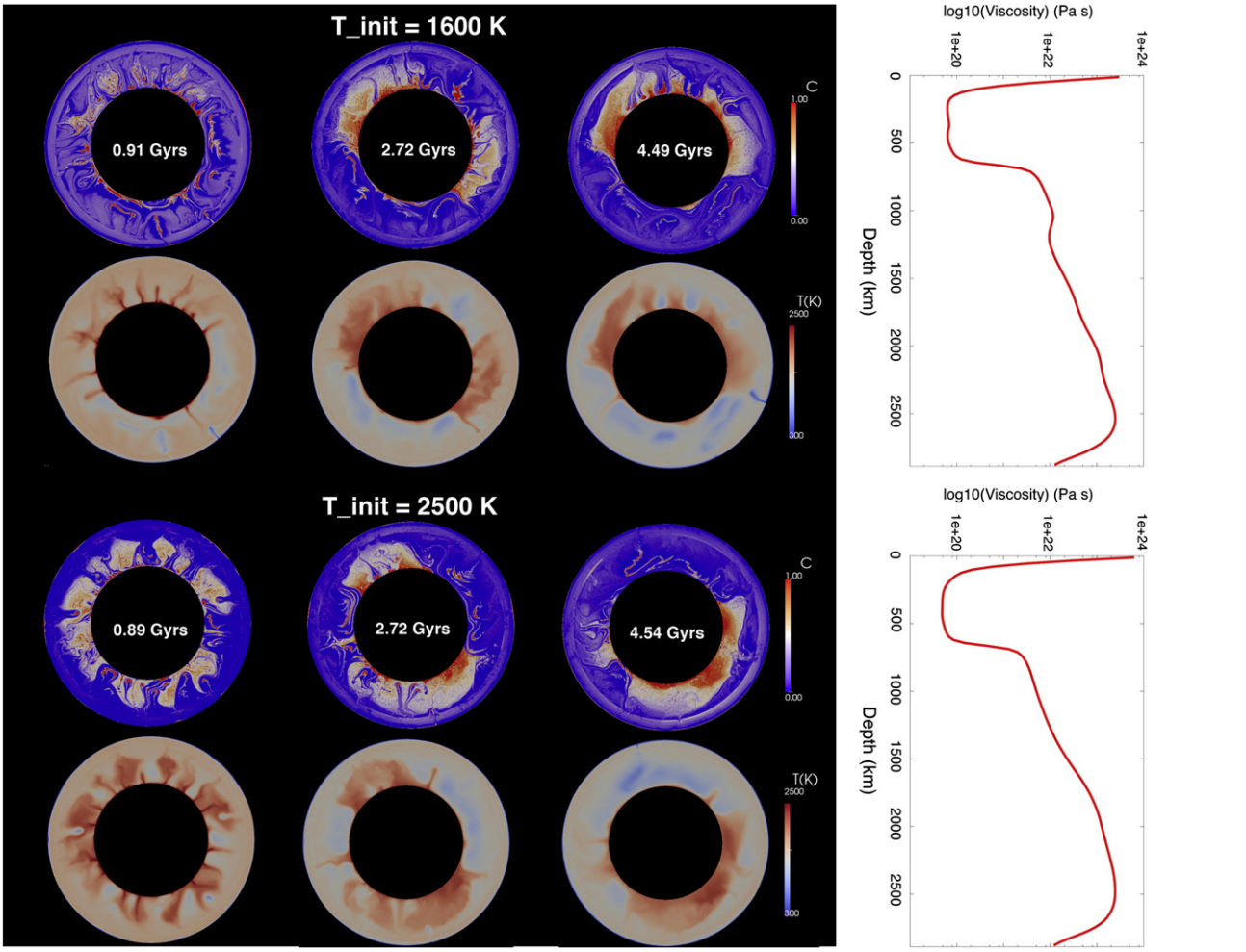

Fig. 1. Time evolution of thermo-chemical structures for cases with a low initial mantle temperature (top), a high initial mantle temperature (bottom) and BSE radiogenic heat production. Time increases from left to right. Viscosity profiles for the final snap shots are plotted on the right.

dynamo activity) found in our previous mantle–core evolution calculations (Nakagawa and Tackley, 2010). All physical parameters are listed in Table 1.

When magmatism is included there are two mechanisms of heat loss across the surface: convective and magmatic. Magmatic heat loss has two components: latent heat and cooling of the solidified basalt. It is instructive to estimate how important this is on the present-day Earth. An upper bound estimate comes from assuming that the basalt cools to the surface temperature, which gives $Q_e = \int \rho \dot{m} \left[C_p(T - T_s) + \mathrm{L}\right] dV$ where L is the latent heat, $\dot{m}$ is the fractional rate of melt generation and Ts is the surface temperature. Oceanic crust is presently produced over an area of 2.9 km^2/yr (e.g. Phipps Morgan (1998)); assuming a thickness of 8 km and a density of 3000 $\mathrm{kg/m}^3$ leads to 2.2×10^6 kg/yr of MORB production. Latent heat release (assuming a latent heat of 500 kJ/kg) thus accounts for 1.1 TW, and magma cooling (from 1600 K minus adiabatic cooling of 200 K (McKenzie and Bickle, 1988) to 300 K with a specific heat capacity of 1200 J/kg/K) accounts for 2.9 TW, a total of 4 TW, which is almost 9% of the total heat loss. For the case of spreading centre volcanism it might instead be considered that cooling is included in the usual half-space cooling solution rather than the magmatic heat loss, leading to a lower bound of 1.1 TW. Assuming a linear initial temperature profile in the oceanic crust (McKenzie et al., 2005) is half way between these bounds. In contrast, for intraplate volcanism such as flood basalts, basalt cooling is certainly part of the magmatic term and needs to be added to the conductive heat flow. In the simulations in this paper, to avoid having to distinguish between spreading centre volcanism and intraplate volcanism, we uniformly quote the upper bound, which does not change the calculated *total* heat flow (or thermal evolution), only the way that it is decomposed into convective and magmatic components.

Two initial mantle potential temperatures are assumed, namely 1600 K (similar to the present-day potential temperature of the shallow mantle (Jaupart et al., 2007)) and 2500 K. The initial temperature profile is adiabatic (assuming solid state) plus thin thermal boundary layers at the surface and CMB. Our model parameterisation is not capable of treating the magma ocean that would in reality result from a surface temperature of 2500 K (Abe, 1997); instead this simply

Table 1
Mantle model physical parameters. $Ra_0 = \rho_0 g \alpha_0 \Delta T_{sa} \mathrm{d}^3 / \kappa_0 \eta_0$.

Symbol	Meaning	Non-D. value	Dimensional value
Ra_0	Rayleigh number	10^7	N/A
η_0	Reference viscosity	1	1.4×10^{22} Pa s
$\Delta\eta$	Viscosity jump at 660 km	30	N/A
σ_b	Yield stress at surface	1×10^5	117 MPa
σ_d	Yield stress gradient	4×10^5	162.4 Pa m^{-1}
ρ_0	Reference (surface) density	1	3300 kg m^{-3}
g	Gravity	1	9.8 m s^{-2}
α_0	Ref. (surface) thermal expan.	1	5×10^{-5} K^{-1}
κ_0	Ref. (surface) thermal diff.	1	7×10^{-7} m^2 s^{-1}
ΔT_{sa}	Temperature scale	1	2500 K
T_s	Surface Temperature	0.12	300 K
L_m	Latent Heat	0.2	6.25×10^5 J kg^{-1}
τ	Half-life	0.00642	2.43 Gyr

causes a short-lived phase of massive magmatism resulting in a highly processed early mantle, in contrast to the low initial T case in which magmatism develops gradually. The chemical composition C, which represents the MORB fraction, is initially uniform at C = 0.2, which is consistent with the amount of MORB that can be generated in a pyrolitic composition (Xu et al., 2008). Three different values of mantle radiogenic internal heating rate are assumed: (1) The value of 28.5 TW obtained by matching the surface heat flow with an assumed Urey ratio (Schubert et al., 2001), here referred to as the "Textbook" value, (2) Bulk Silicate Earth (BSE; 20 TW) (McDonough and Sun, 1995) and (3) BSE with heat-producing elements in the continental crust extracted (7.5 TW (Rudnick and Gao, 2003)), giving 12.5 TW in the mantle. These values are within of range of the heat production determined by observations of geoneutrinos (The KamLand Collaboration, 2011).

We thus introduce a Urey ratio for each heat loss mechanism (convective and magmatic), given as follows:

$$\mathrm{Ur_c} = \frac{\mathrm{R_H M}}{\mathrm{Q_s S_m}}, \mathrm{Ur_e} = \frac{\mathrm{R_H M}}{\mathrm{Q_e S_m}} \tag{2}$$

where $\mathrm{Ur_c}$ is the convective Urey ratio, $\mathrm{Ur_e}$ is the magmatic Urey ratio, $\mathrm{Q_S}$ is the surface heat flux, $\mathrm{Q_e}$ is the eruptive surface heat flux, $\mathrm{R_H}$ is the total heat production rate in the mantle, M is the mass of mantle and $\mathrm{S_m}$ is the surface area of mantle. Using total surface heat flux, which is $\mathrm{Q} = \mathrm{Q_s} + \mathrm{Q_e}$, the total Urey ratio can be defined as

$$\mathrm{Ur} = \frac{\mathrm{R_H M}}{\mathrm{Q}} = \frac{\mathrm{R_H M}}{(\mathrm{Q_s} + \mathrm{Q_e})\mathrm{S_m}} = \left(\frac{1}{\mathrm{Ur_c}} + \frac{1}{\mathrm{Ur_e}}\right)^{-1} \tag{3}$$

where Ur is the total Urey ratio.

The heat production rate decays with time, and is locally dependent on fraction of basaltic material C

$$R_H = H_0\left(\frac{1 + (H_c - 1)C}{1 + (H_c - 1)\langle C\rangle}\right)\exp\left[\frac{(t_a - 1)\ln 2}{\tau}\right] \tag{4}$$

where H_0 is the present-day heating rate, H_c is the ratio of heat production rate in basalt to heat production rate in harzburgite, t_a is the age of the Earth, $\langle C\rangle$ *is the mean basalt fraction* and τ is the averaged half-life of heat production, taken to be 2.43 Gyr. The basalt/harzburgite partitioning factor is a free parameter, taken to be 1, 10 and 100 to check the sensitivity of thermal evolution scenarios to this. The latter factors correspond to relative (to the average) heat-producing element concentrations in (basalt, harzburgite) of (3.6, 0.36) and (4.8, 0.048) respectively.

We here analyse 10 cases with different combinations of total mantle heat production, initial mantle temperature, and basalt heating enhancement.

3. Results

3.1. Effect of initial mantle temperature

Fig. 1 shows thermo-chemical structures as a function of time and 1-D viscosity profiles at the final time snap shot for both low and high initial mantle temperatures and BSE heat production rate. At the earliest time (t = 0.9 Gyr) the compositional fields are very different. The high initial temperature case has already experienced massive melting, crustal production and crustal recycling, resulting in a highly depleted upper ~half of the mantle and a large amount of basalt in the lower ~60% of the mantle. The low initial temperature case, in contrast, has undergone only gradual melting and differentiation, with most of the mantle still primordial but some basalt and harzburgite in the deep mantle. As time progresses, however, the compositional structures become more similar, with large-scale dense piles above the CMB, of which there are sometimes two and sometimes one. Viscosity profiles indicate that for both cases the upper mantle viscosity is about 10^{20} Pa s and the lower mantle viscosity ranges from 10^{23} to 10^{24} Pa s, values that are in the range of estimates from inversion of post-glacial rebound, geoid and other data (Barnhoorn et al., 2011; Haskell, 1935; Mitrovica and Forte, 2004; Peltier, 1996).

The time evolution of convective surface heat flux and volume-averaged mantle temperature are shown in Fig. 2. In the low initial mantle temperature case, the convective surface heat flux is roughly constant with time, with superimposed fluctuations due to episodicity in plate-like behaviour and/or magmatism. In contrast, the high initial temperature case has a surface heat flux that decreases monotonically (with fluctuations), but by 4.5 Gyr the convective heat flux has converged to a similar value in both cases, and this value is close to the constrained value by Jaupart et al. (2007) (32 TW), for which the contribution of heat production in the continental crust is removed. The amplitude of time variations of the surface heat flow over the last few 100 Myr is about ±5 TW. The time evolution of volume-averaged mantle temperature is quite different for the first ~1.5 Gyr. In the low initial temperature case the mantle heats up during this period, whereas in the high initial temperature case there is initially very rapid cooling from ~3000 to ~2600 K due to massive melting and magmatism, followed by a monotonic decrease. After 1.5 Gyr the mantle temperature evolution is very similar in both the cases. The initial temperature rise in the low initial temperature case occurs because internal heating is high whereas convective activity is slow due to the low temperature hence high viscosity.

The heat budget is analysed in left side of Fig. 3. In both cases, there are times when magmatism carries a larger amount of heat flow than thermal conduction through the surface, particularly at early times. Magmatic heat transfer is high when the mantle temperature is high, which occurs in both cases but particularly in the high initial temperature case. Large pulses in magmatic heat flow are observed; these pulses of magmatism are due to time variation in the surface plate motion and also plumes. As in Fig. 2 the surface heat flow is close to be constant for the case with a low initial mantle temperature but monotonically decreases for the case with a high initial

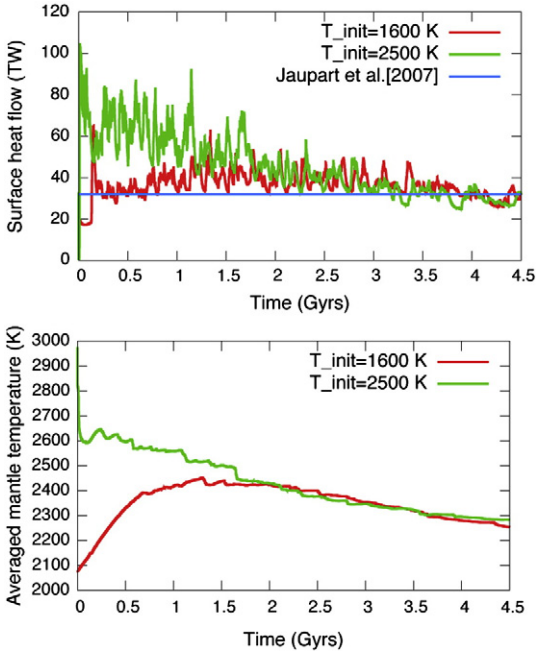

Fig. 2. Surface heat flux (top) and volume-averaged mantle temperature (bottom) as a function of time for the cases in Fig. 1. The blue line in the surface heat flux profile indicates the constraint provided by Jaupart et al. (2007), which is 32 TW.

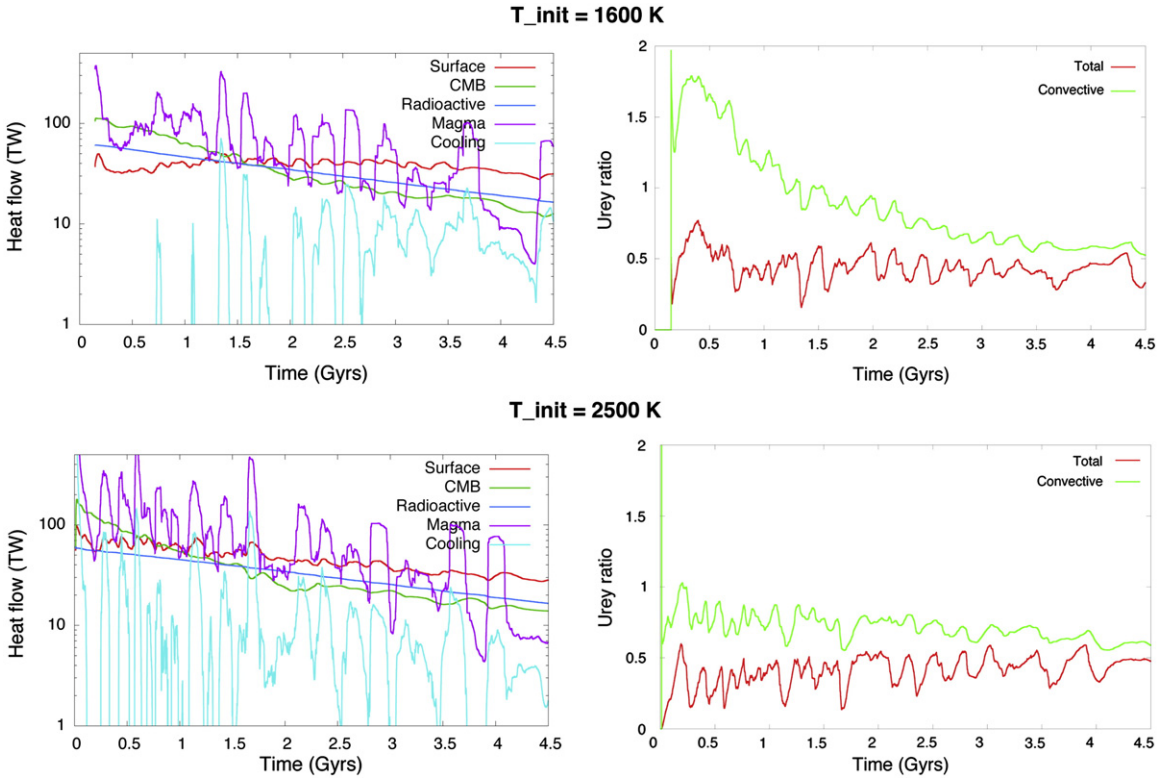

Fig. 3. Contributions to the heat budget (left) and Urey ratios (right) for the cases in Figs. 1 and 2. Top: Case with low initial mantle temperature. Bottom: Case with high initial mantle temperature.

mantle temperature. The core is an important contributor to the global heat budget, with a contribution that is often comparable to radiogenic heating, with present-day CMB heat flow in the range of 10 to 15 TW. In the latter half of the calculation, mantle secular cooling also contributes substantially to the heat budget.

The right side of Fig. 3 shows the Urey ratios as a function of time. For both cases, the Urey ratio that is calculated purely from convective heat flow is always higher than 0.5, similar to what was obtained in previous studies of convective heat transport, which did not consider melt-induced differentiation and thermo-chemical effects (Butler, 2009; Deschamps et al., 2010). As discussed earlier, the actual Urey ratio for Earth is in the range of 0.21 to 0.49. When magmatic heat flow is included (as it should be), the Urey ratio is much lower at early times and slightly lower at the present day, better matching the constraint. The total Urey ratio is roughly constant with time (plus small-timescale fluctuations) in the range of 0.3–0.5. Thus, including magmatism in the present-day heat flow helps in matching the constrained range of values (Jaupart et al., 2007). Note that our simulations do not include continental lithosphere, which is thought to have an important effect on heat transport (e.g. Lenardic et al., 2011).

3.2. Effect of internal heating rate

Fig. 4 shows thermo-chemical structures at t = 4.5 Gyr for the cases with a high initial mantle temperature and the three different internal heating rates. The structures look qualitatively similar for BSE and Textbook, but for BSE–CC the dense piles above the CMB appear smaller and there are more of them.

Fig. 5 shows convective heat flux and volume-averaged mantle temperature as a function of time. The surface heat flow is only slightly different between the three cases, with fluctuations being larger than any systematic difference, and all converge to roughly the observational constraint (32 TW) at the present day. The temperature evolution is, however, quite different between the different cases, with a higher rate of cooling and hence a lower present-day temperature for the cases with a lower internal heating rate. Thus, a lower internal heating rate is compensated, to some extent, by more rapid cooling.

Fig. 6 shows the heat budget and Urey ratios as functions of time. In the heat budget profiles, magmatism again strongly affects heat transport and the mantle cooling rate. The CMB heat flow is typically larger than the radiogenic heating rate for BSE–CC but drops below the radiogenic heating rate for BSE and Textbook cases. Regarding the Urey ratio, including magmatic heat transport strongly decreases the Urey ratio compared to including only conduction, but the values do depend on internal heating rate, with higher heating rate leading to a higher Urey ratio. The total Urey ratio is also affected, although less so, by internal heating rate and at 4.5 Gyr is in the range of 0.4–0.5 for all cases. For BSE–CC the total Urey ratio is close to the convective Urey ratio at t = 4.5 Gyr because magmatism is low, as is realistic for present-day Earth.

3.3. Effect of heat-producing element partitioning

Thermo-chemical structures at t = 4.5 Gyr for cases with different partitioning of heat-producing elements into the basaltic material, a BSE total heating rate and high initial temperature are shown in Fig. 7. The main features are qualitatively not very different between these three cases, but increasing heat concentration into the basaltic material appears to result in fewer piles of basalt above the CMB, which are also larger and hotter. With higher partitioning of heat-producing elements, a larger area of the CMB is left uncovered, allowing plumes to form. In the case with the highest partitioning, two plumes form at the edge of piles, consistent with observational constraints (Thorne et al., 2004; Torsvik et al., 2006) and some previous numerical simulations (Tan et al., 2011).

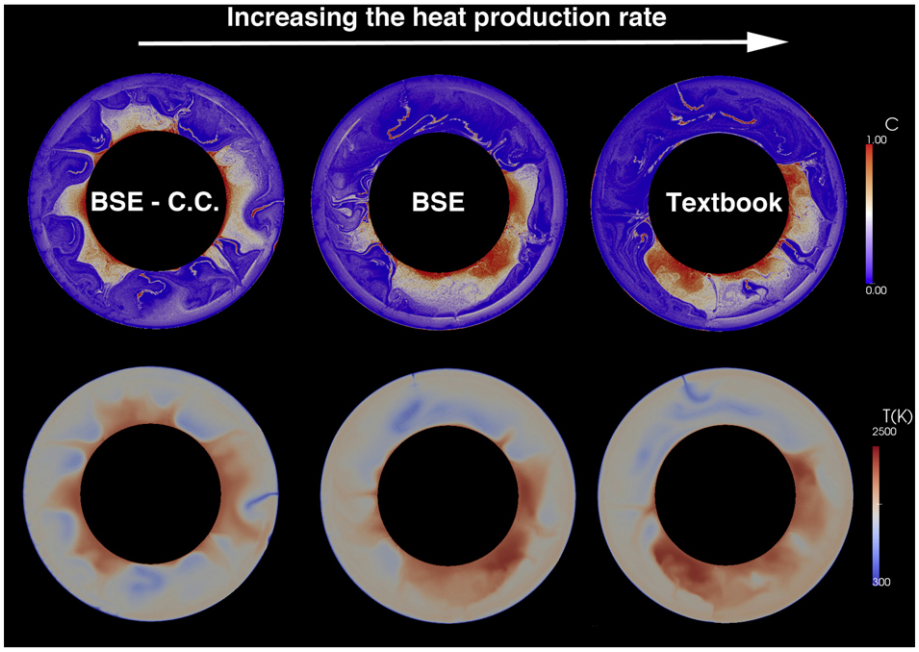

Fig. 4. Thermo-chemical structures at 4.5 Gyr for cases with three different values of internal heat production and high initial temperature. From left to right: BSE–CC, BSE and Textbook. Top: compositional field. Bottom: temperature field.

The time evolution of surface heat flow and volume-averaged mantle temperature are plotted in Fig. 8. The values and the time evolution of surface heat flux are fairly similar for the three heat partition factors, and after 4.5 Gyr are close to the observed 32 TW, but the evolution of volume-averaged mantle temperature is quite different. Higher concentration of *heat production rate* into basaltic material results in lower mantle temperatures. This temperature difference develops between about 0.3 Gyr and 1.2 Gyr into the evolution then remains roughly constant, diminishing towards the end. This appears to be related to a higher rate of magmatism during the early phase, as discussed in the next paragraph.

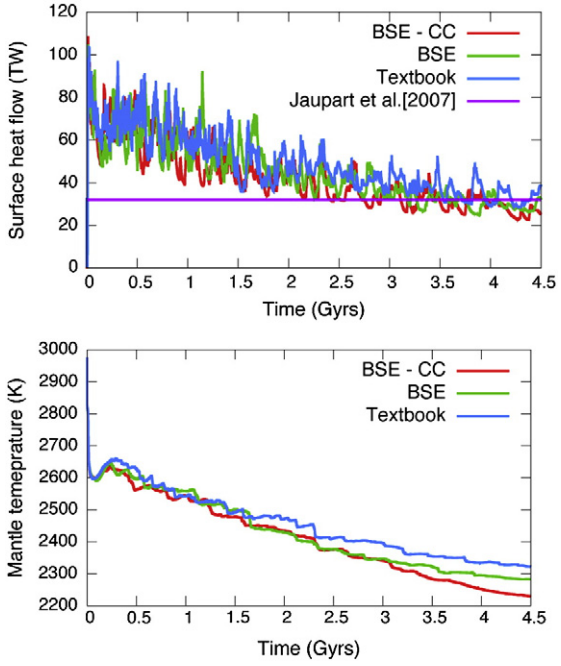

Fig. 5. Time evolution of surface heat flow (top) and volume-averaged mantle temperature (bottom) for cases with three different values of heat production and high initial mantle temperature.

The heat budget and Urey ratios as a function of time for three different rates of enhancement are plotted in Fig. 9. The convective surface heat flow and the CMB heat flow are not sensitive to the heat partitioning. The magmatic heat flow is usually not much different except that it is significantly larger during the early phase (~0.3–1.2 Gyr) for cases with higher partitioning, which results in the divergence of volume-averaged temperature noted for Fig. 8. As a result of the cases having similar surface heat flows, the Urey ratio is not much different, except that the total Urey ratio is slightly lower during the early phase of the high heat partitioning case.

4. Discussion

4.1. Influence of magmatism

The presented calculations indicate that magmatism is an important heat transport mechanism, particularly at early times. As discussed earlier, for present-day Earth, magmatism contributes an upper bound of 9% of the total heat transport. Early parameterized models of Davies (1990) predicted that magmatism can be important for Earth's heat loss, but it has largely been ignored by the Earth mantle modelling community, with a few exceptions. Xie and Tackley (2004) found magmatic heat transport to be the most important heat transport mechanism at early times in thermo-chemical convection models. In models of early Mars, Keller and Tackley (2009) found that magmatism has a dramatic buffering effect on early mantle temperature, causing cases with differing initial temperatures to converge to the same value that is much lower than obtained without magmatism, an effect subsequently termed the “thermostat effect” in the martian evolution models of Ogawa and Yanagisawa (2011). The influence of magmatism is explicitly explored here in supplemental material.

Thermal evolution modelling using fully dynamical convection simulations exhibited a Urey ratio of around 0.6 (Butler, 2009), while statistically steady-state, isoviscous calculations suggested 0.4 to 0.6 (Deschamps et al., 2010). These values are higher than the 0.21–0.49 indicated by geophysical and geochemical constraints (Jaupart et al., 2007). The convective Urey ratio (i.e. not including magmatic heat transport) found in the present study is similar to

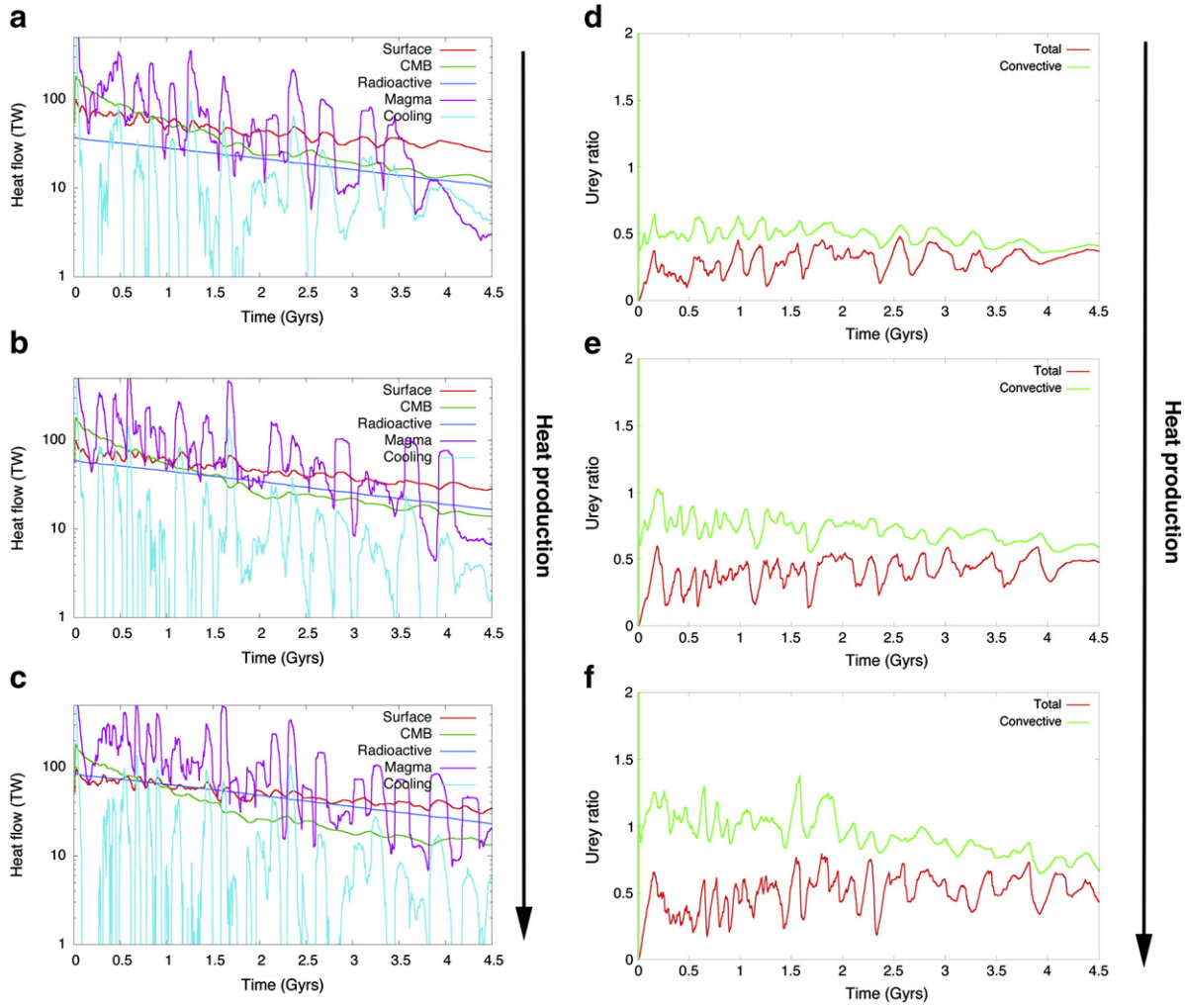

Fig. 6. Heat budget contributions (left) and Urey ratios (right) as a function of time for cases with three different values of heat production and high initial mantle temperature (2500 K). (a) and (d): BSE–CC. (b) and (e): BSE. (c) and (f): Textbook.

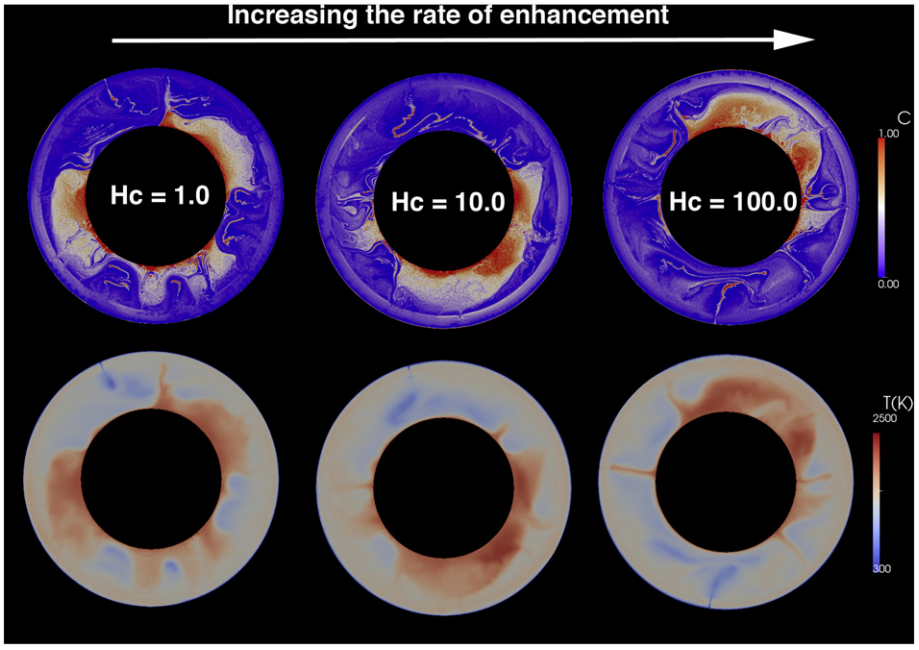

Fig. 7. Thermo-chemical structures after 4.5 Gyr for cases with three different partitioning of heat production into the basaltic material. The total amount of heat production is BSE value and the initial mantle temperature is high (2500 K). Top: compositional field. Bottom: temperature field.

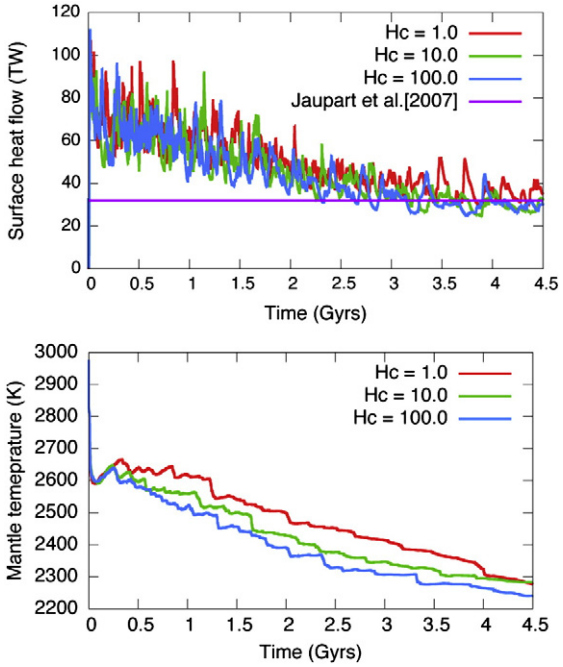

Fig. 8. Surface heat flow (top) and volume-averaged mantle temperature (bottom) as a function of time for the cases in Fig. 8 with different partitioning of internal heating into basaltic material.

that found in these simple numerical models, but when magmatic heat transport is included the present-day Urey ratio decreases to the range of 0.4–0.5, which is at the upper end of the constrained value.

4.2. Possible influence of continents

The heat production rate in continental crust has some uncertainty, with a plausible range of 6 to 8 TW. Based on numerical simulations, Lenardic et al. (2011) conclude that the mantle heat flow would be roughly the same if continents were removed and their heat sources mixed into the mantle, which would shift the Urey ratio to the range of 0.33–0.76, a range that encompasses our present models as well as previous numerical models. This argument does not consider the fact that in these two scenarios the contributions from core cooling and mantle cooling would be different, resulting in a different thermal history, but the influence of this is difficult to assess without detailed study.

4.3. Early Earth

After the moon-forming giant impact the mantle was likely completely molten (e.g. Benz and Cameron, 1990; Stevenson, 2007); its subsequent history is one of cooling and solidification, starting with solidification of the magma ocean (Abe, 1997; Solomatov, 2007). Recently it was proposed that in addition to a surface magma ocean, a basal magma ocean existed in the deep mantle and continued for a geologically long period (Labrosse et al., 2007). Our current model parameterization is not capable of treating magma oceans, but the high initial mantle temperature cases here are intended to, in a crude way, emulate the rapid near-surface magmatic processing of the mantle that likely took place in early times and was, for example, considered by Davies (1990) in developing scalings for heat loss by magmatism. Modelling internal magmatic processing, such as that related to a Basal Magma Ocean (Labrosse et al., 2007) or "upside-down differentiation" (Lee et al., 2010) is beyond the scope of the present model. While the resulting mantle structure is quite different from cases with a low initial temperature early in the simulation, after 4.5 Gyr of evolution the structures look very similar, meaning that present-day mantle structure is not a good constraint on early evolution. Other observations must be used to constrain processes in the early Earth that can be tested with numerical mantle convection simulations.

4.4. Potential energy release due to basalt segregation

The energy balance graphs do not include potential energy release due to the settling of dense basalt above the CMB, so it is worth performing a rough estimate of this. Within the assumptions of the present model (total volume fixed, gravitational acceleration constant in radius and time), the change in mantle potential energy for the extreme case of going from a uniform mantle to one with all the basalt (20%) in a layer above the CMB and all the harzburgite above it can be straightforwardly calculated. If the basalt-harzburgite density difference is 200 kg/m^3 and the energy release is spread out over 4.5 Gyr, the average power release is 0.76 TW, which is small compared to the other heat budget contributions. In contrast, for example, a decrease in mean temperature of 100 K/Gyr releases about 15 TW.

4.5. Mantle cooling rate

Another constraint on the thermal evolution of Earth's mantle is the cooling rate inferred from petrological studies. Abbott et al. (1994) found that the mantle cooling rate from the Archean to present is in the range of 60 to 80 K/Gyr, and Herzberg et al. (2010) obtained an estimate consistent with the upper end of this range. The cooling rate of volume-averaged temperature predicted from our simulations can be inferred from Figs. 2, 5 and 8, and is around 70 K/Gyr. Hence, it appears to be consistent with the petrological estimates. Note that the petrological estimates are for the shallow mantle but the temperature in our figures is averaged over the whole mantle. In a future study we will make a more detailed comparison.

5. Conclusions

Here we investigate the influence of initial mantle temperature, internal heating rate and partitioning of heat-producing elements into basaltic material on the thermo-chemical evolution of the Earth's mantle. The main findings are as follows:

1. The present-day surface heat flow, to a first approximation, does not depend on the initial mantle temperature or partitioning of heat-producing elements into basalt, and is weakly dependent on the exact value of internal heating rate. The value of surface heat flux obtained in all cases in this study is close to the observationally-constrained value of 32 TW (Jaupart et al., 2007). Along similar lines, in our previous paper on the thermal evolution of Earth's core (Nakagawa and Tackley, 2010) it was found that the present-day state hardly depends on initial core temperature.
2. Thermal and chemical structures after 4.5 Gyr of evolution are not sensitive to the initial mantle temperature, even though early thermo-chemical structures depend strongly on initial temperature. However, they are slightly changed by the heat production rate and the partitioning of heat-producing elements into basalt.
3. Magmatism is an important heat loss mechanism for much of the planet's history. From the figures showing heat budget contributions (Figs. 3, 6 and 9), it is clear that magmatic heat flow is the dominant heat loss mechanism at early times. For the present-day Earth, mid-ocean ridge magmatism accounts for an upper bound of 9% of the heat loss. Pulses of magmatism cause rapid cooling.
4. Accounting for magmatic heat loss reduces the calculated Urey ratio, by a large amount at early times, with all cases being in the range of 0.4–0.5 at the present day, which is at the upper end of the constrained range. The present-day surface convective heat flux

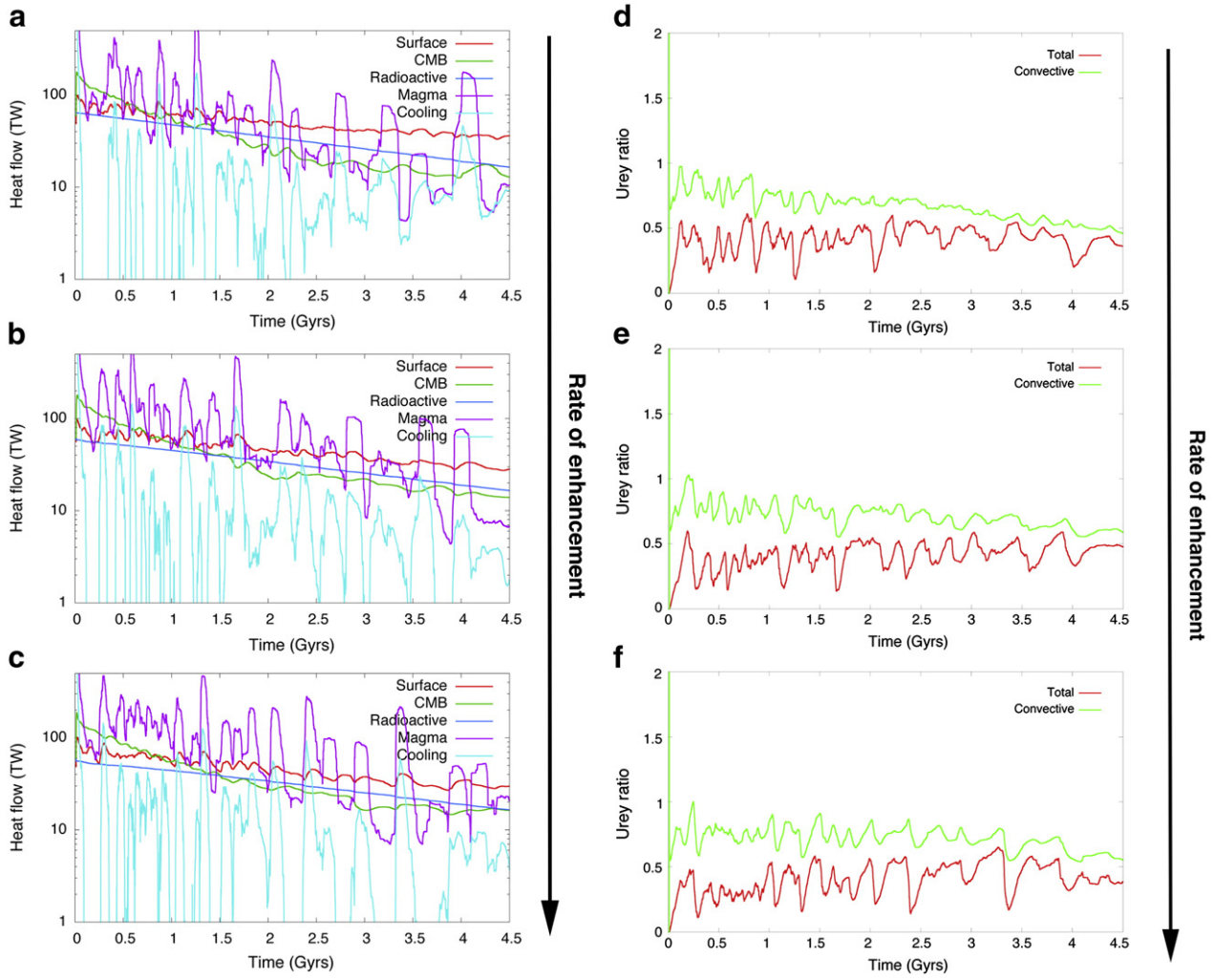

Fig. 9. Heat budget contributions (left) and Urey ratios (right) as a function of time for the cases in Figs. 8 and 9 with different partitioning of heat production rate into basaltic material. (a) and (d): Hc = 1. (b) and (e): Hc = 10. (c) and (f): Hc = 100.

in all cases converges to about 32 TW, but higher internal heating rate leads to higher magmatic heat transport to be added to this. Nevertheless it appears that Earth's surface heat flux can be explained even if the Urey ratio is higher than some authors have suggested.

5. Since in the present study the present-day surface heat flow is weakly changed by changing various parameters including internal heating rate, the calculated Urey ratio is quite dependent on the total heat production in the mantle. The mantle heat production has huge uncertainties: observations of geoneutrinos indicate a wide range of 10–30 TW (The KamLand Collaboration, 2011) while geochemical analyses variously indicate a Urey ratio between 0.08 and 0.49 (Jaupart et al., 2007; Lyubetskaya and Korenaga, 2007; McDonough and Sun, 1995). In contrast, the surface heat flow is reasonably well constrained, at least at the present day. Therefore, it is better for numerical convection (or thermal evolution) models to attempt to match the surface heat flow rather than the Urey ratio.

Supplementary materials related to this article can be found online at doi:10.1016/j.epsl.2012.02.011.

Acknowledgements

Numerical simulations were performed on the Brutus cluster managed by the HPC team at ETH Zurich and the SGI Altix JAMSTEC Supercomputer system. Author thanks Shijie Zhong and two anonymous reviewers for valuable comments that help to improve the original manuscript.

References

Abbott, D., Burgess, L., Longhi, J., Smith, W.H.F., 1994. An empirical thermal history of the Earth's upper mantle. J. Geophys. Res. 99, 13835–13850.
Abe, Y., 1997. Thermal and chemical evolution of the terrestrial magma ocean. Phys. Earth Planet. Inter. 100, 27–39.
Barnhoorn, A., van der Wal, W., Vermeersen, B.L.A., Druty, M.R., 2011. Lateral, radial, and temporal variations in upper mantle viscosity and rheology under Scandinavia. Geochem. Geophys. Geosyst. 12 (Q01007). doi:10.1029/2010GC003290.
Benz, W., Cameron, A.G.W., 1990. Terrestrial effects of the giant impact. In: Newsom, H.E., Jones, J.H. (Eds.), Origin of the Earth. Oxford University Press, New York, pp. 61–68.
Buffett, B.A., Heuret, A., 2011. Curvature of subducted lithosphere from earthquake locations in the Wadati-Benioff zone. Geochem. Geophys. Geosyst. 12 (Q06110). doi:10.1029/2011GC003570.
Butler, S.L., 2009. Effects of phase boundary induced layering on the Earth's thermal history. Geophys. J. Int. 179, 1330–1340.
Christensen, U.R., 1985. Thermal evolution models for the earth. J. Geophys. Res. Solid Earth Planets 90, 2995–3007.
Coltice, N., Ferrachat, S., Ricard, Y., 2000. Box modeling the chemical evolution of geophysical systems: case study of the Earth's mantle. Geophys. Res. Lett. 27, 1579–1582.
Conrad, C.P., Hager, B.H., 1999. The thermal evolution of an Earth with strong subduction zones. Geophys. Res. Lett. 26, 3041–3044.
Davaille, A., 1999. Simultaneous generation of hotspots and superswells by convection in a heterogeneous planetary mantle. Nature 402, 756–760.
Davies, G.F., 1980. Thermal histories of convective Earth models and constraints on radiogenic heat production in the Earth. J. Geophys. Res. 85, 2517–2530.

Davies, G.F., 1990. Heat and mass transport in the early Earth. In: Newsome, H.E., Jones, J.H. (Eds.), Origin of the Earth. Oxford University Press, New York, pp. 175–194.
Davies, G.F., 2009. Effect of plate bending on the Urey ratio and the thermal evolution of the mantle. Earth Planet. Sci. Lett. 287, 513–518.
Deschamps, F., Tackley, P.J., Nakagawa, T., 2010. Temperature and heat flux scalings for isoviscous thermal convection in spherical geometry. Geophys. J. Int. 182, 137–154.
Gonnermann, H.M., Manga, M., Jellinek, A.M., 2002. Dynamics and longevity of an initially stratified mantle. Geophys. Res. Lett. 29, 1399.
Grigne, C., Labrosse, S., Tackley, P.J., 2005. Convective heat transfer as a function of wavelength: Implications for the cooling of the Earth. J. Geophys. Res. 110. doi:10.1029/2004JB003376.
Grigne, C., Labrosse, S., Tackley, P.J., 2007. Convection under a lid of finite conductivity in wide aspect ratio models: effects of continents on the wavelength of mantle flow. J. Geophys. Res. 112 (B08403). doi:10.1029/2006JB004297.
Gurnis, M., 1989. A reassessment of the heat-transport by variable viscosity convection with plates and lids. Geophys. Res. Lett. 16, 179–182.
Haskell, N.A., 1935. The motion of a viscous fluid under a surface load. Physics 6, 265–269.
Hernlund, J.W., Tackley, P.J., 2008. Modeling mantle convection in the spherical annulus. Phys. Earth Planet. Inter. 171, 48–54.
Herzberg, C., Condie, K., Korenaga, J., 2010. Thermal history of the Earth and its petrological expression. Earth Planet. Sci. Lett. 292, 79–88.
Honda, S., Iwase, Y., 1996. Comparison of the dynamic and parameterized models of mantle convection including core cooling. Earth Planet. Sci. Lett. 139, 133–145.
Jaupart, C., Labrosse, S., Mareschal, J.-C., 2007. Temperature, heat and energy in the mantle of the Earth. Treatise on Geophysics, vol 7: Mantle dynamics, pp. 253–303.
Keller, T., Tackley, P.J., 2009. Towards self-consistent modeling of the martian dichotomy: the influence of one-ridge convection on crustal thickness distribution. Icarus 202, 429–443.
Korenaga, J., 2006. Archean Geodynamics and the thermal evolution of Earth: AGU monograph series, 164, pp. 7–32.
Korenaga, J., 2008. Urey ratio and the structure and evolution of Earth's mantle. Rev. Geophys. 46 (R2007). doi:10.1029/2007RG000241.
Korenaga, J., 2010. Scaling of plate tectonic convection with pseudoplastic rheology. J. Geophys. Res. 115 (B11405). doi:10.1029/2010JB007670.
Labrosse, S., Jaupart, C., 2007. Thermal evolution of the Earth: secular changes and fluctuations of plate characteristics. Earth Planet. Sci. Lett. 260, 465–481.
Labrosse, S., Hernlund, J.W., Coltice, N., 2007. A crystallizing dense magma ocean at the base of the Earth's mantle. Nature 450, 866–869.
Lee, C.-T., Luffi, P., Hoink, T., Li, J., Dasgupta, R., Hernlund, J., 2010. Upside-down differentiation and generation of a 'primordial' lower mantle. Nature (UK) 463, 930–933.
Lenardic, A., Cooper, C.M., Moresi, L., 2011. A note on continents and the Earth's Urey ratio. Phys. Earth Planet. Inter. 188, 127–130.
Leng, W., Zhong, S., 2010. Constraints on viscous dissipation of plate bending from compressible mantle convection. Earth Planet. Sci. Lett. 297, 154–164.
Lyubetskaya, T., Korenaga, J., 2007. Chemical composition of Earth's primitive mantle and its varience: 1. Method and results. J. Geophys. Res. 112 (B03211). doi:10.1029/2005JB004223.
McDonough, W.F., Sun, S.-S., 1995. The composition of the Earth. Chem. Geol. 120, 223–253.
McKenzie, D., Bickle, M.J., 1988. The volume and composition of melt generated by extension of the lithosphere. J. Petrol. 29 (3), 625–679.
McKenzie, D., Jackson, J., Priestley, K., 2005. Thermal structure of oceanic and continental lithosphere. Earth Planet. Sci. Lett. 233, 337–349.
Mitrovica, J.X., Forte, A.M., 2004. A new inference of mantle viscosity based upon joint inversion of convection and glacial isostatic adjustment data. Earth Planet. Sci. Lett. 225, 177–189.
Nakagawa, T., Tackley, P.J., 2004. Effects of thermo-chemical convection on thermal evolution of the Earth's core. Earth Planet. Sci. Lett. 220, 207–219.
Nakagawa, T., Tackley, P.J., 2005. Deep mantle heat flow and thermal evolution of Earth's core in thermo-chemucal multiphase models of mantle convection. Geochem. Geophys. Geosyst. 6. doi:10.1029/2005GC000967.
Nakagawa, T., Tackley, P.J., 2010. Influence of initial CMB temperature and other parameters on the thermal evolution of Earth's core resulting from thermo-chemical spherical mantle convection. Geochem. Geophys. Geosyst. 11 (Q06001). doi:10.1029/2010GC003031.
Nakagawa, T., Tackley, P.J., 2011. Effects of low-viscosity post-perovskite on thermo-chemical mantle convection in a 3-D spherical shell. Geophys. Res. Lett. 38 (L04309). doi:10.1029/2010GL046494.
Ogawa, M., 2007. Superplumes, plates, and mantle magmatism in two-dimensional numerical models. J. Geophys. Res. 112 (B06404). doi:10.1029/2006JB004533.
Ogawa, M., Yanagisawa, T., 2011. Numerical models of martian mantle evolution induced by magmatism and solid-state convection beneath stagnant lithosphere. J. Geophys. Res. 116. doi:10.1029/2010JE00377.
Peltier, W.R., 1996. Mantle viscosity and ice-age ice-sheet topography. Science 273, 1359–1364.
Phipps Morgan, J., 1998. Thermal and rare gas evolution of the mantle. Chem. Geol. 145, 431–445.
Rudnick, R.L., Gao, S., 2003. The composition of the continental crust. In: Holland, H., Turekian, K.K. (Eds.), Treatise on Geochemistry, vol. 3. Elsevier, pp. 1–64.
Schubert, G., Turcotte, D.L., Olson, P., 2001. Mantle Convection in the Earth and Planets. Cambridge Uni. Press, New York.
Solomatov, V.S., 2007. Magma oceans and primordial mantle differentiation. In: Schubert, G. (Ed.), Treatise on Geophysics, vol. 9, pp. 91–120.
Stevenson, D.J., 2007. Earth formation and evolution. In: Stevenson, D.J. (Ed.), Treatise on Geophysics. Elsevier B. V., Amsterdam, pp. 1–11.
Tackley, P.J., 2008. Modelling compressible mantle convection with large viscosity contrasts in a three-dimensional spherical shell using the yin-yang grid. Phys. Earth Planet. Inter. 171, 7–18.
Tan, E., Land, W., Zhong, S., Gurnis, M., 2011. On the location of plumes and lateral movement of thermochemical structures with high bulk modulus in the 3-D compressible mantle. Geochem. Geophys. Geosyst. 12 (Q07005). doi:10.1029/2011GC003665.
The KamLand Collaboration, 2011. Partial radiogenic heat model for Earth revealed by geoneutrino measurements. Nature Geoscience 4, 647–651.
Thorne, M.S., Grand, S.P., Garnero, E.J., 2004. Geographic correlation between hot spots and deep mantle lateral shear-wave velocity gradients. Phys. Earth Planet. Inter. 146, 47–63.
Torsvik, T.H., Smethurst, M.A., Burke, K., Steinberger, B., 2006. Large igneous provinces generated from the margins of the large low-velocity provinces in the deep mantle. Geophys. J. Int. doi:10.1111/j.1365-1246X.2006.03158.x.
Turcotte, D.L., 1980. On the thermal evolution of the Earth. Earth Planet. Sci. Lett. 48, 53–58.
Xie, S., Tackley, P.J., 2004. Evolution of U–Pb and Sm–Nd systems in numerical models of mantle convection and plate tectonics. J. Geophys. Res. 109, B11204. doi:10.1029/2004JB003178.
Xu, W.B., Lithgow-Bertelloni, C., Stixrude, L., Ritsema, J., 2008. The effect of bulk composition and temperature on mantle seismic structure. Earth Planet. Sci. Lett. 275, 70–79.